Pergamon

PII: S0301-9322(96)00008-0

Int. J. Multiphase Flow Vol. 22, No. 4, pp. 767–781, 1996

0301-9322/96 $15.00 + 0.00

TRANSIENT EFFECTS OF NUCLEATION IN STEADY AND UNSTEADY CONDENSING FLOWS

C. F. DELALE† and G. H. SCHNERR
Institut für Strömungslehre und Strömungsmaschinen, Universität Karlsruhe (TH), Germany

(Received 12 March 1995; in revised form 30 January 1996)

Abstract—Transient effects of nucleation in steady and unsteady expansions of a vapor in metastable state are investigated in the relaxation time approximation (RTA). Three regions of nucleation with corresponding nucleation times are distinguished for general applications and the unsteady nucleation rate equation is explicitly displayed in each region using an asymptotic method. Applications to shock tube and nozzle experiments for the expansion of moist air show that transient nucleation effects on nucleation rates become more significant near saturation (in the validity of RTA) than near maximum nucleation rates. The position of the nucleation wave front, which corresponds to states of maximum nucleation, on particle paths and the flow field therein seem to be unaltered by transient nucleation effects except for expansions on those particle paths with cooling rates higher than $3°C/\mu s$ near the center of rarefaction waves in shock tubes. Copyright © 1996 Elsevier Science Ltd.

Key Words: transient effects, characteristic nucleation times, relaxation time approximation

1. INTRODUCTION

Two-phase flows with nonequilibrium phase transition are of fundamental importance in science and technology. They arise in very diverse fields such as atmospheric physics, astrophysics, aerophysics, nuclear, chemical and steam turbine technologies, rocketry, etc. In all of these applications a vapor in the metastable state acts as a source for the production of condensation nuclei which grow into droplets during the nonequilibrium transition from the vapor to the liquid phase. The phenomenon of production of condensation nuclei by thermal fluctuations in the vapor phase itself is known as homogeneous nucleation. The kinetics of homogeneous nucleation reaching rapidly a steady nonequilibrium state is described in detail by Zettlemoyer (1969), Abraham (1974), McDonald (1963) and references therein. In general most studies are devoted to the description of steady-state nucleation rate equations. This is because in ordinary experiments such as those encountered in cloud chambers and supersonic nozzles the characteristic time of nucleation is usually too short to be considered. However, for flows with very high cooling rates such as those of supersonic free-molecular jets transient effects become important. Unsteady effects of nucleation were first considered by Zeldovich (1942). He even derived an equation for the unsteady nucleation rate, but his estimate was only qualitative. A number of investigators (e.g. Kantrowitz 1951; Probstein 1951; Wakeshima 1954; Collins 1955; Courtney 1962; Andrés & Boudart 1965; Feder *et al.* 1966) considered the relaxation to steady-state and obtained expressions for the nucleation time lag in order to determine the validity of steady-state rate equations. Only recently has Shneidman (1987) shown that these relaxation rate equations are too simple to account for the complex structure of the relaxation to steady-state. He even achieved a relatively simple expression for the relaxation of the unsteady nucleation to steady-state, but this expression unfortunately relies on the choice of the initial size of incipient nuclei.

In this study transient effects of nucleation in steady and unsteady expansions are investigated in the relaxation time approximation (RTA) of the nucleation rate equation. Despite the fact that the RTA is not valid in the initial nucleation period, initial nucleation rates are vanishingly small

†*Present address*: Department of Mechanical Engineering, University of Istanbul, 34850 Avcılar, Istanbul, Turkey and Department of Mathematics, Research Institute for Basic Sciences, TÜBİTAK—Marmara Research Center, P.O. Box 21, 41470 Gebze, Turkey.

so that they can hardly influence the asymptotic behavior of the RTA which is valid at later times. During the expansion (compression in the case of retrograde fluids) of the vapor in the metastable state, three distinct regions of nucleation are distinguished and the unsteady nucleation rate equation together with the characteristic nucleation times are exhibited in each region in the relaxation time approximation using an asymptotic method. Conditions under which steady-state nucleation rates are reached are also displayed in each region during the expansion. The results are then applied to the experiments in shock tubes and nozzles. It is demonstrated that for these experiments transient effects become more important as the initial stage of nucleation is approached. No influence on the gas dynamical behavior was found for expansions with cooling rates where measurements are possible. The influence of the transient effects on the position of the nucleation wave, constructed from states of maximum nucleation, and on the flow variables therein could only be observed for expansions with very high cooling rates ($>3^{\circ}C/\mu s$) in the shock tube experiments along particle paths very close to the center of the rarefaction wave where measurements are practically impossible.

2. STEADY-STATE NUCLEATION RATE EQUATIONS

It is well known that the crucial point in describing the steady-state current or nucleation rate J'_S is the determination of Gibbs formation energy $\Delta G'_i$ for the creation of a cluster of size i (i-mer). In the metastable state of the vapor, $\Delta G'_i$ shows a maximum ΔG^* at the critical size $i = i^*$. By the stability criterion only clusters exceeding the critical size can grow. It can further be deduced that mainly clusters of critical size contribute to the expression of steady-state nucleation rate. Assuming that clusters and the surrounding vapor have the same temperature T', the isothermal steady-state nucleation rate $(J'_S)_{\text{isothermal}}$ is given by

$$(J'_S)_{\text{isothermal}} = ZD^*n^*. \tag{1}$$

In [1] n^* is the equilibrium number density of clusters of critical size (proportional to the factor $\exp[-\Delta G^*/kT']$ where k is Boltzmann's constant), D^* is the rate of molecular impact on the surface of a cluster of critical size given by the kinetic expression

$$D^* = \frac{p'_v}{\sqrt{2\pi m_1 kT'}} s^* \tag{2}$$

where p'_v denotes the vapor pressure, m_1 is the mass of a single vapor molecule and where s^* denotes the surface area of a critical cluster, and Z is the nonequilibrium Zeldovich factor defined by

$$Z \equiv \sqrt{-\frac{1}{2\pi kT'}\left(\frac{\partial^2 \Delta G'_i}{\partial i^2}\right)_{i=i^*}}. \tag{3}$$

If the Gibbs formation energy of an i-mer is expressed by

$$\Delta G'_i = -ikT' \ln S + \sigma' s'_i \tag{4}$$

where $S \equiv p'_v/p'_\infty(T')$ denotes the supersaturation with $p'_\infty(T')$ corresponding to the saturation pressure at T', s'_i is the surface area of an i-mer and where σ' is the surface tension, we recover the classical nucleation equation (Farkas 1927; Becker & Döring 1935; Volmer 1939; Zeldovich 1942; Frenkel 1946). If, in addition, the translational and rotational contributions are taken into account in [4], we end up with the steady-state nucleation rate equation of Lothe & Pound (1962) which yields nucleation rates far off by orders of magnitude from those predicted by the classical nucleation equation. If [4] for Gibbs formation energy is replaced by Fisher's expression (1967) together with the surface tension correction for small clusters, we obtain the Dillmann–Meier rate equation (1991). A more refined and self-consistent theory by Delale & Meier (1993) accounts in addition for the deviation of the surface area of a cluster from its geometric value. The last two steady-state nucleation equations have been shown to compare reasonably well with experimental measurements for a variety of substances over a wide range of temperatures. An alternative self-consistent theory is also available from the work of Kalikmanov & van Dongen (1995).

All of the above mentioned steady-state nucleation rate equations neglect the heating up of the cluster by impinging molecules. Feder *et al.* (1966) have demonstrated that this effect can simply be taken into account by multiplying the isothermal steady-state equation [1] by a correction factor Φ (for water vapor this factor is approximately 1/5). Thus all of the steady-state nucleation rate equations together with the nonisothermal correction of Feder *et al.* (1966) can now be written as

$$J'_S = \Phi Z D^* n^*. \tag{5}$$

In particular when we exploit the fact that n^* is proportional to $\exp[-\Delta G^*/kT']$, we can cast [5] into the normalized form

$$J_S \equiv \frac{J'_S}{\zeta'} = \Sigma(p'_v, T')\exp[-K^{-1}B(p'_v, T')] \tag{6}$$

where ζ' is a normalization constant chosen such that $\Sigma(p'_v, T')$ is of O(1) numerically and where K, called the nucleation parameter hereafter, and B, called the normalized activation function hereafter, are identified from the relation

$$K^{-1}B(p'_v, T') \equiv \frac{\Delta G^*(p'_v, T')}{kT'} \tag{7}$$

in such a way that $B = O(1)$ numerically over the range where nucleation rates are appreciable (for explicit expressions for K and B of [7] in the classical nucleation theory, see Delale *et al.* 1993, 1995). In particular, as the saturation line is approached, $B \to \infty$. Thus, we have $J_S \equiv 0$ at saturation. On the other hand, the relatively long time interval compared to expansion (compression) time for normal (retrograde) fluids required for nucleation to reach its peak value implies $K \ll 1$. In what follows we employ the normalized form [6] with $K \ll 1$ for the steady-state nucleation rate, independent of any particular choice of nucleation theories.

3. TRANSIENT EFFECTS OF NUCLEATION

The steady-state nucleation rate equations discussed in the preceding section are valid only when all transient effects have disappeared from the system. In general these transient effects persist over a local relaxation time τ', called *the nucleation time lag* or *induction time*. During this period the formation of clusters of size i can be described by a kinetic equation of the Fokker–Planck type (e.g. see Zeldovich 1942) as

$$\frac{\partial c'}{\partial t'} = -\frac{\partial J'}{\partial i}, \quad J' = -D' c'_0 \frac{\partial}{\partial i}\left(\frac{c'}{c'_0}\right) \tag{8}$$

where $c' = c'(i, t')$ is the concentration of clusters of size i at a given time t', $c'_0 = c'_0(i)$ is the corresponding equilibrium concentration, $J'(i, t')$ is the unsteady nucleation rate of clusters of size i at t' and $D' = D'(i)$ is the diffusion coefficient. It is well known that [8] tends to steady-state with a steady-state nucleation rate J'_S.

Zeldovich (1942) was the first to study transient effects of nucleation by [8]. He even achieved an expression for the time lag. Unfortunately, it contained undetermined functions to be evaluated, thus his estimate was only qualitative. Wakeshima (1954) succeeded in finding an explicit expression for time lag, which is simple enough to be written as

$$\tau' = \frac{1}{4\pi D^* Z^2} \tag{9}$$

where D^* is given by [2] and Z is the Zeldovich factor defined by [3]. For typical cloud chamber experiments Wakeshima's time lag estimate is of the order of microseconds. The same order of magnitude estimates were also achieved by Kantrowitz (1951), Probstein (1951) and Collins (1955) which support Wakeshima's estimate given by [9]. It should, however, be mentioned that Wakeshima's estimate is not valid in the very initial period and consequently his form of decay to steady-state is too simplistic. A well-defined estimate of time lag for the isothermal nucleation

equation was derived by Andrés & Boudart (1965) employing the nucleation kinetic equation [8] in difference form. Feder *et al.* (1966) suggest that if one employs the expression

$$(\tau')_{\text{isothermal}} = \frac{1}{2D^*Z^2} \qquad [10]$$

which differs from Wakeshima's expression of [34] by a factor of 2π, one obtains time lag estimates in agreement with the results of Andrés & Boudart (1965). Furthermore, they show how the nonisothermal time lag expression can be related to the isothermal one by simply dividing by the so-called nonisothermal factor Φ, already introduced in [5]. Their final expression for the nonisothermal time lag τ' can be written as

$$\tau' = \frac{(\tau')_{\text{isothermal}}}{\Phi} = \frac{1}{2\Phi D^*Z^2}. \qquad [11]$$

Only recently has Shneidman (1987) shown from the solution of [8] that the decay to steady-state over the period τ' is more complex than the relaxation time approximation (RTA) employed by early investigators. His result in the leading term can be written as

$$J'(t') = J'_S \exp\left\{ -\exp\left(-\frac{t' - t'_i}{\tau'} \right) \right\} \qquad [12]$$

for $t' > t'_i$ where t'_i is some "incubation" time depending on the choice of the incipient nuclei. For $t' < t'_i$ the nucleation rate is practically zero. For sufficiently large times (e.g. $t' \gg t'_i$) [12] approximates to the relaxation rate equation employed by previous investigators. Although [12], to the leading approximation, seems to describe the actual form of decay of [8] to steady-state, it has the disadvantage that it relies upon the choice of the initial size of the incipient nuclei from which the incubation time t'_i can be calculated. Furthermore, [12] is restricted to a fixed thermodynamic state of the vapor since it is obtained from [8] for a fixed thermodynamic state of the vapor. In actual nucleation experiments the thermodynamic state of the vapor is continuously changing.† Nevertheless, aside from certain anomalies near the coexistence or saturation line, [12] can be successfully used to describe the initial nucleation period. For times $t' \gg t'_i$ [12] coincides with the relaxation time approximation (RTA), which in local form can be written as

$$\frac{dJ'}{dt'} = \frac{J'_S - J'}{\tau'}. \qquad [13]$$

In [13] the time derivative d/dt' is the material or total derivative during an expansion (we herein refer to normal fluid behavior. For retrograde fluids the word 'expansion' should be replaced by the word 'compression'). Although [13] is not valid near the initial nucleation period, i.e. for times $t' < t'_i$ and $t' = O(t'_i)$, nucleation rates there are vanishingly small to effect the validity of RTA, [13], for later times. Thus, except for the initial nucleation period, [13] can be conveniently applied to nucleation experiments since it takes into account changes in the thermodynamic state and flow conditions during such experiments. The choice of the initial condition for [13] follows from the fact that $J'_S = 0$ at saturation. If we denote the time at which saturation is reached during the expansion by t'_c (from now on subscript c refers to the saturation state), we have

$$J' = 0 \quad \text{at} \quad t' = t'_c \qquad [14]$$

for the initial condition of [13]. On the other hand, [13] is coupled to the expansion process through the thermodynamic coordinates p'_v and T' which enter the expressions for J'_S and τ'. Thus the solution of the relaxation rate equation [13] subject to the initial condition [14] demands the nature of the expansion process. For most nucleation experiments the expansion is achieved in either unsteady flows (e.g. as in expansion cloud chambers or shock tubes) or steady flows (e.g. as in supersonic nozzle flows). In what follows we present the solution of [13] subject to the initial condition [14] depending on the unsteady or steady nature of the expansions in nucleation experiments.

†In his work Shneidman (1987) has retained these effects as higher approximations, but only for changes in the height of the activation barrier $\Delta G^*/kT'$ by introducing the quantity $n = \tau' \partial/\partial t' \, (\Delta G^*/kT')$.

3.1. *Unsteady expansions*

Before we consider the solution of [13], we introduce the normalized variables

$$t \equiv \frac{t'}{\Theta'}, \quad \tau \equiv \frac{\tau'}{\Theta'} \tag{15}$$

where Θ' is some characteristic flow time for the expansion. We also define

$$J \equiv \frac{J'}{\zeta'}, \quad J_S \equiv \frac{J'_S}{\zeta'} \tag{16}$$

where ζ' is a conveniently chosen normalization constant for nucleation. Equation [13] now assumes the normalized form

$$\frac{dJ}{dt} = \frac{J_S - J}{\tau} \tag{17}$$

subject to the initial condition $J = 0$ at $t = t_c$, whose solution can be immediately written as

$$J(t) = \int_{t_c}^{t} J_S(t_1) \frac{\exp\left[-\int_{t_1}^{t} \frac{dv}{\tau(v)} \right]}{\tau(t_1)} dt_1 \tag{18}$$

along particle paths during expansions. Now using [6] for J_S, we arrive at

$$J(t) = \int_{t_c}^{t} \frac{\Sigma(t_1)\exp[-K^{-1}B(t_1)]}{\tau(t_1)} \exp\left[-\int_{t_1}^{t} \frac{dv}{\tau(v)} \right] dt_1 \tag{19}$$

where it is understood that the thermodynamic state of the vapor, characterized by the relations $p'_v = p'_v(t)$ and $T' = T'(t)$ at any time t along particle paths during an expansion, is known from the nature of the expansion. The nucleation rate equation [19] along particle paths in an expansion is essentially influenced by the behavior of the normalized activation function B. A typical time variation of the activation function B along particle paths during an expansion is shown in figure 1 where it is also compared with its virtual isentropic variation $B_{\text{isentropic}}$. It can clearly be seen that B is minimum at its turning point $t = t_l$, which corresponds to a maximum nucleation rate, where

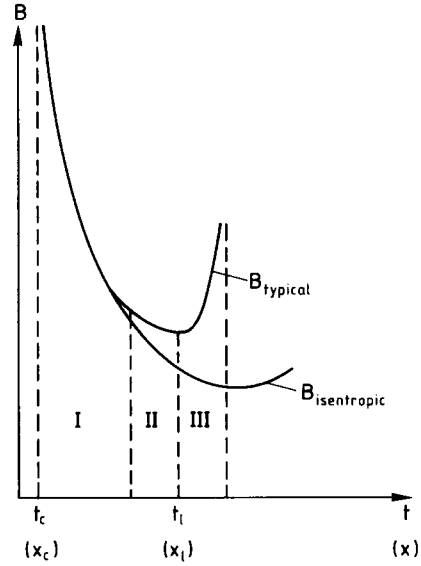

Figure 1. Typical history of the normalized activation function B along particle paths (t_c and x_c denote, respectively, the time and position where saturation conditions are reached in, respectively, unsteady and steady expansions, t_l and x_l are the corresponding time and position where the nucleation rate reaches its maximum value).

$dB/dt \equiv 0$. Since the nucleation parameter $K \ll 1$, we distinguish from the behavior of the normalized activation three distinct regions of nucleation (Regions I, II and III) along particle paths during an expansion.

In Region I, $dB/dt = O(1)$ numerically. Using Laplace's method (e.g. see Erdelyi 1956; Sirovich 1971) in the limit as $K \to 0$ where the essential contribution to the integral [19] arises from the end point minimum $t_1 = t$, we obtain the following asymptotic expression for the unsteady nucleation rate equation in Region I at any instant t along particle paths:

$$J(t) = \hat{\Sigma}(t)\exp[-K^{-1}B(t)] \tag{20}$$

where

$$\hat{\Sigma}(t) \equiv \Sigma(t)\frac{\{1-\exp[-(1+\tau(t)/\tau^*(t))(t-t_c)/\tau(t)]\}}{[1+\tau(t)/\tau^*(t)]} \tag{21}$$

with the normalized characteristic time for steady-state nucleation in this region given by

$$\tau^* \equiv -K\left(\frac{dB}{dt}\right)^{-1}. \tag{22}$$

Region II is defined as the region where $dB/dt = O(K^{1/2})$ on measure K. In this region the nucleation rate still increases ($dB/dt < 0$), but at a slower rate until it peaks at the turning point of the activation function, which also marks the end of the region. Using Laplace's method for an end-point minimum as $K \to 0$ in this region, we obtain the simple asymptotic expression for $J(t)$ as

$$J(t) = \bar{\Sigma}(t)\exp[-K^{-1}B(t)] \tag{23}$$

where $\bar{\Sigma}(t)$ is now given by

$$\bar{\Sigma}(t) = \Sigma(t)\left\{\frac{1}{2}\sqrt{\frac{\pi}{C(t)}}\frac{\exp[A^2(t)/(4C(t))]}{\tau(t)}\right.$$
$$\left.\times\left[\operatorname{erfc}\left(\frac{A(t)}{2\sqrt{C(t)}}\right)-\operatorname{erfc}\left(\sqrt{C(t)}(t-t_c)+\frac{A(t)}{2\sqrt{C(t)}}\right)\right]\right\} \tag{24}$$

with

$$A(t) \equiv \left[\frac{1}{\tau(t)}+\frac{1}{\tau^*(t)}\right] \tag{25}$$

$$C(t) \equiv \frac{1}{2}\left[\frac{1}{\tau^{**2}(t)}+\frac{d\tau/dt}{\tau^2(t)}\right] \tag{26}$$

erfc denoting the complementary error function and where the characteristic time for steady-state nucleation of this region is defined by

$$\tau^{**} \equiv K^{1/2}\left(\frac{d^2B}{dt^2}\right)^{-1/2}. \tag{27}$$

In particular as $t \to t_l$, $\tau^* \to \infty$ and we obtain the maximum nucleation rate $J_{max} = J_l$ where it is understood that subscript l denotes properties or functions evaluated at $t = t_l$. Finally, we define Region III as that region where the nucleation rate starts to decrease from its maximum value and consequently where we have $dB/dt > 0$ (see figure 1). This region begins at $t = t_l$ along particle paths and ends at a point where nucleation has diminished for all practical purposes. Solving [17] subject to the condition $J = J_l$ at $t = t_l$ and using Laplace's method now for an interior minimum, we obtain the asymptotic expression for the unsteady nucleation rate in the form

$$J(t) = J_l\exp\left[-\frac{(t-t_l)}{\tau_l}\right]$$
$$\times\left\{\frac{1+\operatorname{erf}[\sqrt{C_l}(t-t_l)-A_l/(2\sqrt{C_l})]-\operatorname{erfc}[\sqrt{C_l}(t_l-t_c)+A_l/(2\sqrt{C_l})]}{\operatorname{erfc}[A_l/(2\sqrt{C_l})]-\operatorname{erfc}[\sqrt{C_l}(t_l-t_c)+A_l/(2\sqrt{C_l})]}\right\} \tag{28}$$

for $t > t_l$ along particle paths. It is worthwhile to mention that in [28], A_l and C_l are now respectively given by [25] and [26] evaluated at $t = t_l$ and erf and erfc, respectively, denote the error function and the complementary error function. Furthermore, it can easily be deduced from [28] that as $t \to t_l$, $J \to J_l$ and as $t \to \infty$, $J \to 0$.

Having exhibited the asymptotic expressions for unsteady nucleation rates in the distinct Regions I, II and III, it would be interesting to find out the validity of steady-state nucleation rates. In Region I it can easily be demonstrated from [21] that $\hat{\Sigma}(t)$ approaches $\Sigma(t)$, thus nucleation rates approach steady-state along particle paths if, at each instant t, we can satisfy the conditions

$$\tau(t) \ll \tau^*(t) \quad \text{and} \quad \tau(t) \ll (t - t_c). \tag{29}$$

The second condition is usually automatically satisfied in the RTA which holds for times larger than t_c. In Region II it can be deduced from [24] that time lag effects become unimportant whenever the conditions

$$\left(\frac{\tau(t)}{\tau^{**}(t)}\right)^2 + \frac{d\tau}{dt} \ll 1 \quad \text{and} \quad \tau(t) \ll \tau^*(t) \tag{30}$$

are satisfied at each instant t along particle paths. As $t \to t_l$ in this region, $\tau^* \to \infty$. Thus the second condition of [30] is automatically satisfied. In particular at $t = t_l$ where the nucleation rate is maximum, unsteady effects are insignificant whenever

$$\left(\frac{\tau_l}{\tau_l^{**}}\right)^2 + \left(\frac{d\tau}{dt}\right)_l \ll 1. \tag{31}$$

It can further be shown that [31] also exhibits the condition for the validity of steady-state nucleation theory in Region III along particle paths in unsteady expansions.

3.2. Steady expansions

In steady expansions of nucleating flows, which are usually encountered in supersonic nozzles and wind tunnels, we first note that the relaxation rate equation [13] assumes the form

$$\frac{dJ'}{dx'} = \frac{J'_S - J'}{L'} \tag{32}$$

with

$$L' \equiv u'\tau' \tag{33}$$

where x' is a characteristic streamwise coordinate (or axial coordinate in one-dimensional flows), u' is the local flow speed and τ' is the time lag for nucleation. The length L' given by [33] is a measure of a characteristic local length over which unsteady effects prevail. This length will be referred to as the *nucleation distance lag* or the *nucleation induction distance*. Carrying out the normalization for nucleation rates given by [16] together with the introduction of the normalized variables

$$x \equiv \frac{x'}{l'} \quad \text{and} \quad L \equiv \frac{L'}{l'} \tag{34}$$

where l' is a characteristic flow length, we obtain the relaxation differential equation

$$\frac{dJ}{dx} = \frac{J_S - J}{L} \tag{35}$$

subject to the initial condition $J = 0$ at $x = x_c$ (subscript c herein also refers to saturation conditions). It is obvious from [35] that unsteady nucleation rates completely relax to steady ones ($J \to J_S$) as $L \to 0$, which corresponds to $\tau' \to 0$. The solution of [35] subject to vanishing nucleation rate at saturation can now be written as

$$J(x) = \int_{x_c}^{x} \Sigma(x_1)\exp[-K^{-1}B(x_1)] \frac{\exp\left[-\int_{x_1}^{x} \frac{d\xi}{L(\xi)}\right]}{L(x_1)} dx_1. \tag{36}$$

Similar to the procedure of unsteady flows, the integral of [36], as $K \to 0$, is dominated by the behavior of the normalized activation function whose variation along the streamwise coordinate x is shown in figure 1. Once again we can distinguish three distinct regions. Region I is defined as that region where $dB/dx = O(1)$ numerically, Region II is defined as the region where $dB/dx = O(K^{1/2})$ and Region III is defined as that region where the nucleation rate decreases ($dB/dx > 0$) in contrast to Regions I and II where the nucleation rate increases ($dB/dx < 0$). The point $x = x_l$, which marks the end of Region II, again corresponds to the point where the nucleation rate is maximum. If we define the characteristic steady-state nucleation lengths $L^*(x)$ and $L^{**}(x)$ of Region I and II by

$$L^*(x) \equiv -K\left(\frac{dB}{dx}\right)^{-1} \qquad [37]$$

and

$$L^{**}(x) \equiv K^{1/2}\left(\frac{d^2B}{dx^2}\right)^{-1/2} \qquad [38]$$

the asymptotic expressions for the nucleation rates in Regions I, II and III are exactly those given, respectively, by [20]–[28] provided that the time coordinate t is replaced by the streamwise coordinate x and the following correspondence is strictly observed:

$$\tau(t) \leftrightarrow L(x)$$

$$\tau^*(t) \leftrightarrow L^*(x)$$

and

$$\tau^{**}(t) \leftrightarrow L^{**}(x).$$

The conditions in each region, under which steady-state nucleation rates are valid, can then be obtained from [29]–[31] by observing the above correspondence between time and length variables strictly.

4. APPLICATIONS TO CONDENSING SHOCK TUBE AND NOZZLE FLOW EXPERIMENTS

In this section we apply the results of the previous section for unsteady and steady expansions of water vapor with a carrier gas in shock tubes and nozzles to determine the transient effects of nucleation quantitatively. Although it is well known (e.g. see Kotake & Glass 1981) that, for the available measured data typical of such experiments, the transient effects of nucleation do not affect the gas dynamical behavior (the quasi-steady assumption), it is interesting to compare the steady and unsteady nucleation rates and the characteristic times in distinct nucleation regions. Furthermore, the transient effects of nucleation on the gas dynamical behavior (in particular, on the flow field near maximum nucleation rates) can be studied theoretically in the shock tube experiments along particle paths having very high cooling rates where measurements are practically impossible.

As an example of unsteady expansions, we consider the homogeneous nucleation of water vapor in the rarefaction wave of a shock tube whose wave diagram is shown in figure 2. As the mixture of water vapor and carrier gas (air), which for time $t' < 0$ is at rest in the driver section (region 4 in figure 2) with initial relative humidity φ_4, initial specific humidity ω_4 and initial temperature T'_4, expands into the channel (Region 1 in figure 2) after the rupture of the diaphragm, the water vapor is cooled in metastable state where homogeneous nucleation sets in until condensation becomes visible at high supersaturation ratios due to significant number of droplets formed (onset of condensation). The curve EF in the x'–t' diagram of figure 2, called the nucleation wave front, corresponds to states where maximum nucleation rates are reached along different particle paths. The waves emanating from the center O of the rarefaction wave remain almost straight as long as they do not cross the nucleation wave front EF; however, as they cross the nucleation wave front EF, they begin to curve appreciably towards the head of the rarefaction wave due to substantial latent heat release by condensation. The curve OMP in figure 2 shows such a typical wave.

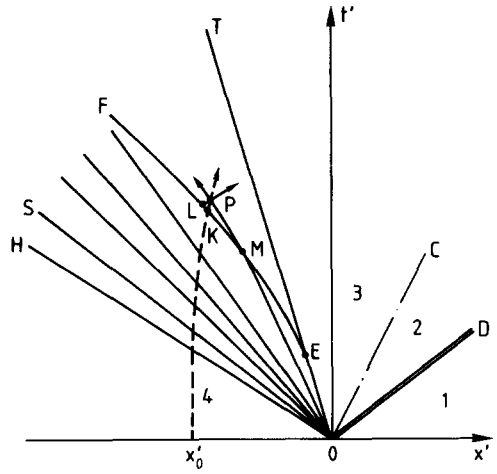

Figure 2. Wave diagram for shock tube flows with homogeneous condensation (OH and OT are, respectively, the isentropic head and tail of the rarefaction wave travelling to the left, OD is the shock wave travelling to the right, OC is the contact surface, OS is the wave along which saturation conditions are reached, EF is the nucleation wave front defined as the locus of states of maximum supersaturation or maximum nucleation rate, the dashed line is a typical particle path originally located at x'_0, Regions 4 and 1 correspond to the initial states of the driver section and of the channel, respectively).

Homogeneous nucleation practically sets in along a particle path (dashed line in figure 2 initially located at x'_0) as soon as it crosses the saturation wave OS. At point K, where the particle path meets the nucleation wave front, the nucleation rate reaches its maximum value $J_{max} = J_l$. The nucleation rate then decreases along KP until it completely diminishes. We herein investigate the transient effects of nucleation on the nucleation rate as well as on the position of the nucleation wave front EF and on the flow variables therein. For this reason we choose to consider these effects along particle paths where measured data are available (e.g. Barschdorff 1975), which unfortunately show relatively low cooling rates, as well as along those particle paths with very high cooling rates close to the center O where measurements are practically impossible. In determining the state of the vapor (p'_v, T') along the particle path and in constructing the nucleation wave front, it is

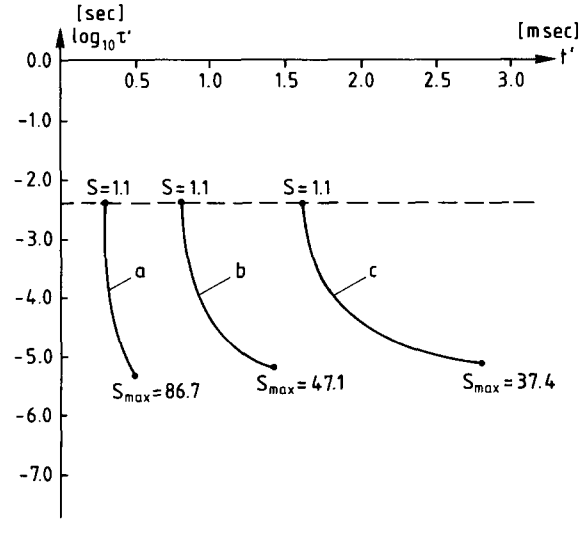

Figure 3. Variation of the time lag expression given by [11] along different particle paths in the shock tube experiments of Barschdorff (1975) for the expansion of moist air (S denotes the supersaturation with maximum value S_{max}; initial driver conditions are: mixture pressure $p'_4 = 790.6$ Torr, partial vapor pressure $(p'_v)_4 = 4.3$ Torr and mixture temperature $T'_4 = 297.2$ K; the calculated value of the nucleation parameter is $K = 0.875 \times 10^{-2}$). (a) Expansion along particle path initially at $x'_0 = -5$ cm; (b) expansion along particle path initially at $x'_0 = -20$ cm; (c) expansion along particle path initially at $x'_0 = -40$ cm.

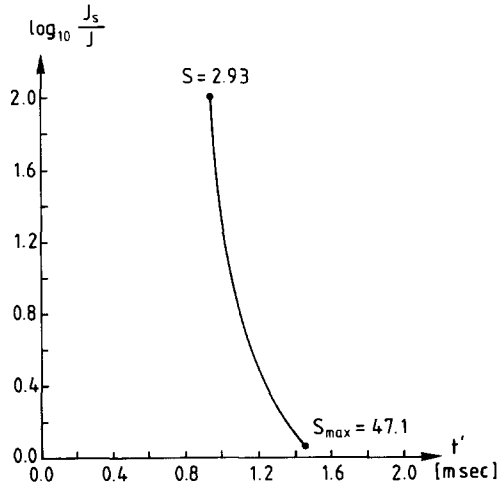

Figure 4. Ratio of steady-state to unsteady nucleation rates in Barschdorff's shock tube experiments (1975) under the conditions stated along a particle path initially at $x_0' = -20$ cm corresponding to curve b of figure 3 (S denotes supersaturation with maximum value S_{max}).

important that a precise gas dynamical solution is used. We therefore use the recent asymptotic solution of Delale *et al.* (1995). Furthermore, we employ the classical steady-state nucleation theory discussed in section 2 together with the Hertz–Knudsen law for the growth of critical nuclei into droplets (this latter law is needed for the construction of the nucleation wave front EF. Details of normalization of the nucleation and growth laws together with the thermodynamic properties used can be found in Delale *et al.* 1995). For the time lag expression, we use that given by [11] together with the value $\Phi = 1/5$ for water vapor suggested by Feder *et al.* (1966). Figure 3 shows typical orders of magnitude for the nucleation time lag τ' given by [11] along different particle paths (curves *a*, *b* and *c*) during the expansion of moist air in the experiments of Barschdorff (1975). It can clearly be seen that τ' changes by orders of magnitude during the expansion along any of the particle paths. While τ' is of the order of milliseconds near saturation ($S = 1.1$), it decreases to the order of microseconds near the peak of nucleation ($S = S_{max}$). This suggests that transient effects on the nucleation rate are less significant as maximum nucleation rates are approached along particle paths. This fact is also demonstrated in figure 4 during the expansion along a particle path where the ratio of the steady-state to the unsteady nucleation rates is shown. The difference

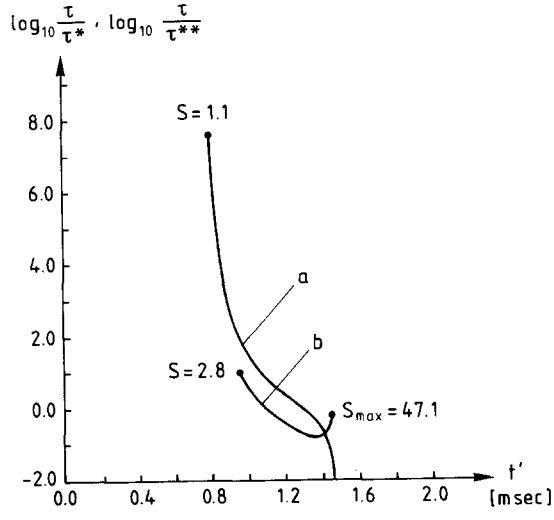

Figure 5. Comparison of the ratios of the time lag τ to the characteristic times τ^* and τ^{**} of Regions I and II in Barschdorff's shock tube experiments (1975) under the conditions along a particle path initially at $x_0' = -20$ cm corresponding to curve b of figure 3 (S denotes supersaturation with maximum value S_{max}). (a) Variation of $\log_{10} \tau/\tau^*$ along the particle path; (b) variation of $\log_{10} \tau/\tau^{**}$ along the particle path.

Table 1. The effect of nucleation time-lag on the flow variables at maximum nucleation in the classical nucleation theory for the expansion of moist air along a particle path originally at $x_0' = -4$ mm in Barschdorff's experiments (1975) with initial driver section conditions given in figure 3

Flow variables	Steady-state nucleation	Unsteady nucleation
p_l' (Pa)	24771	24523
T_l' (K)	196.57	196.01
u_l' (m/s)	323.3	325.3
t_l' (μs)	40.01	40.36
J_l' ($m^{-3} s^{-1}$)	4.41×10^{26}	4.15×10^{26}
$S_l = S_{max}$	495.3	525.1

becomes almost negligible near the maximum nucleation rate. Typical variations of the ratios of time lag τ to the characteristic nucleation times τ^* and τ^{**} of Regions I and II during an expansion along the same particle path are also exhibited in figure 5. The position of the nucleation wave front and the gas dynamical variables therein, as expected, seem to be unaltered by transient effects of nucleation during the expansion along particle paths initially located at $x_0' = -5$, -20 and -40 cm (having cooling rates of 0.28, 0.07 and 0.04°C/μs, respectively). In order to be able to observe the influence of nucleation time lag on the flow field near maximum nucleation rates under the same initial driver section conditions, one should really consider expansions along those particle paths with very high cooling rates. Although it is possible to achieve the desired cooling rates on particle paths very close to the center O, no measurement is practically possible along these particle paths. Nevertheless, the information gained from such theoretical calculations can show when transient effects of nucleation begin to influence the position of the nucleation wave front and the flow variables therein under the same initial conditions. For this reason we consider the expansion along a particle path initially at $x_0' = -4$ mm with a high cooling rate of 3°C/μs, where the transient effects of nucleation begin to influence the position of the nucleation wave front and the flow variables therein. A comparison of the flow variables at maximum nucleation rates using the classical steady-state and the corresponding unsteady nucleation rate equations under the same initial driver section conditions (stated in figure 3) is shown in table 1. The transient effects seem to result in a delay for the position of the nucleation wave front on the particle path with a slight

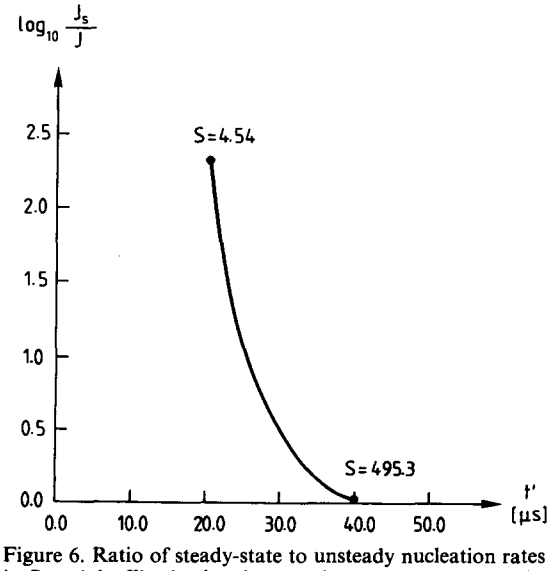

Figure 6. Ratio of steady-state to unsteady nucleation rates in Barschdorff's shock tube experiments (1975) under the conditions stated in figure 3 along a particle path initially at $x_0' = -4$ mm (S denotes supersaturation).

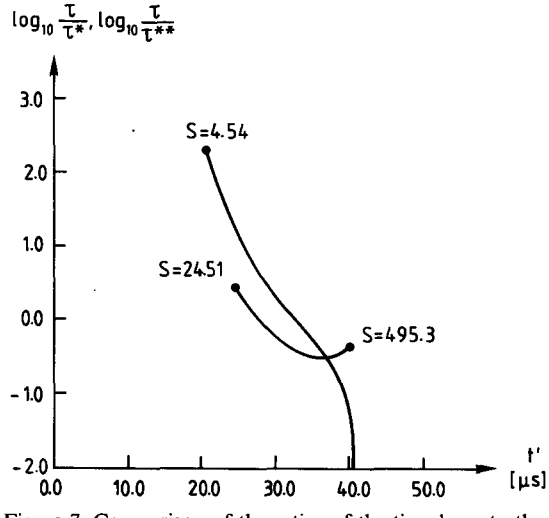

Figure 7. Comparison of the ratios of the time lag τ to the characteristic times τ^* and τ^{**} of Regions I and II in Barschdorff's shock tube experiments (1975) under the conditions stated in figure 3 along a particle path initially at $x_0' = -4$ mm (S denotes supersaturation). (a) Variation of $\log_{10} \tau/\tau^*$ along the particle path; (b) variation of $\log_{10} \tau/\tau^{**}$ along the particle path.

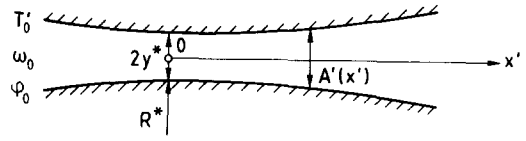

Figure 8. Geometric configuration of a circular arc nozzle with throat height $2y^*$ and circular arc radius R^*.

decrease in the temperature and pressure therein. There is a slight increase in the maximum nucleation rate despite a noticeable increase in the maximum supersaturation ratio. The ratio of the steady-state to unsteady nucleation rates along the same particle path is plotted in figure 6. This also shows that transient effects on nucleation rates are more appreciable as saturation is approached, a typical behaviour reached on all particle paths. The ratios of the time lag τ to the characteristic times of nucleation in Regions I and II along the same particle path are also exhibited in figure 7. All of these results demonstrate that, for the specified initial driver section conditions, transient effects of nucleation would begin to influence the position of the nucleation wave front and the flow variables therein only along those pathlines having cooling rates greater than $3°C/\mu s$.

To determine transient effects of nucleation in steady expansions, we choose to work with one-dimensional steady condensing nozzle flows for which a precise asymptotic theory by Delale *et al.* (1993) is available. We consider the expansion of moist air with reservoir temperature T_0', reservoir specific humidity ω_0 and reservoir relative humidity φ_0 in a converging–diverging circular arc nozzle, whose geometric configuration is shown in figure 8. The water vapor reaches the saturation state in the converging section and maximum nucleation rates are achieved during the transonic expansion of the vapor in metastable state. We investigate transient nucleation effects on steady-state nucleation rates as well as on the position of the nucleation wave, constructed from states of maximum nucleation, and the flow field therein. We once more use the nonisothermal classical steady-state nucleation equation given by [5] together with the Hertz–Knudsen droplet growth law and the time lag expression given by [11]. Details of the method together with the

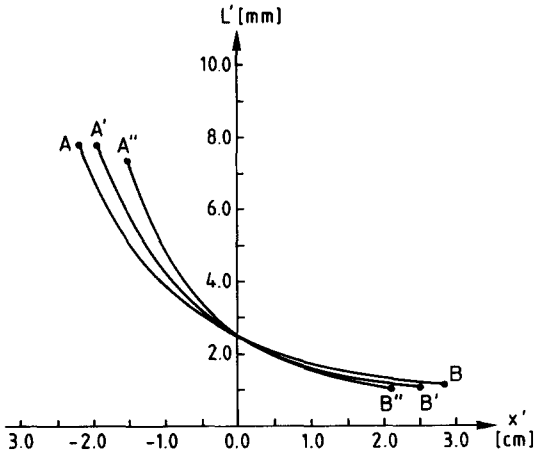

Figure 9. Variation of the characteristic length scale L' defined by [33], where the time lag τ' is given by [11], along the nozzle axis in Schnerr's experiments (1989) for moist air expansions with fixed reservoir conditions: temperature $T_0' = 295.6$ K, specific humidity $\omega_0 = 6.5$ g/kg, relative humidity $\varphi_0 = 0.38$ and with fixed throat height $2y^* = 30$ mm, but variable circular arc radius R^* yielding different expansion rates (AB corresponds to an expansion rate with $R^* = 400$ mm and with supersaturations $S_A = 2.52$ and $S_B = S_{max} = 66.5$; $A'B'$ corresponds to an expansion rate with $R^* = 300$ mm and with supersaturations $S_{A'} = 2.52$ and $S_{B'} = S_{max} = 71.0$; $A''B''$ corresponds to an expansion rate with $R^* = 200$ mm and with supersaturations $S_{A''} = 2.60$ and $S_{B''} = S_{max} = 77.8$).

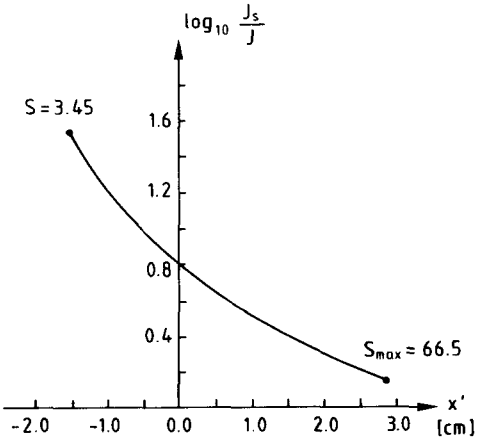

Figure 10. Ratio of steady-state to unsteady nucleation rates in Schnerr's nozzle experiments (1989) under the conditions stated in figure 7 along the S2 nozzle axis with $R^* = 400$ mm and $2y^* = 30$ mm corresponding to the expansion AB in figure 7 (S denotes supersaturation with maximum value S_{max}).

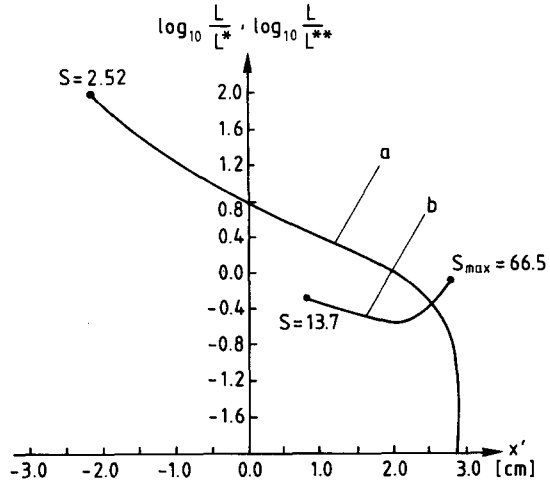

Figure 11. Comparison of the ratios of the distance lag L to the characteristic lengths L^* and L^{**} of Regions I and II in Schnerr's nozzle experiments (1989) under the conditions stated in figure 7 along the S2 nozzle axis with $R^* = 400$ mm and $2y^* = 30$ mm corresponding to the expansion AB in figure 7 (S denotes supersaturation with maximum value S_{max}). (a) Variation of $\log_{10} L/L^*$ along the nozzle axis; (b) variation of $\log_{10} L/L^{**}$ along the nozzle axis.

thermodynamic properties employed can be found in Delale *et al.* (1993). Figure 9 shows typical magnitudes of the distance lag L', defined by [33], for the expansion of moist air with reservoir conditions $\varphi_0 = 0.38$, $\omega_0 = 6.5$ g/kg, $T_0' = 295.6$ K in nozzles having the same throat height ($2y^* = 30$ mm), but with different radii corresponding to different expansion rates (expansions AB, $A'B'$ and $A''B''$, where points B, B' and B'' correspond to states of maximum supersaturations, are achieved in nozzles with circular arc radii $R^* = 400$, 300 and 200 mm having approximate cooling rates of 0.3, 0.35 and 0.43°C/μs, respectively). The higher values of L' achieved near saturation (points A, A' and A'') suggest that transient effects are more significant near saturation. Figure 10 shows the variation of the ratio of steady to unsteady nucleation rates under the same reservoir conditions in the circular arc nozzle with throat height $2y^* = 30$ mm and $R^* = 400$ mm (expansion AB in figure 9). This confirms that transient effects on nucleation rates are more significant near the saturation state rather than near maximum nucleation. The variations in the ratios of the normalized nucleation distance lag to the characteristic lengths L^* and L^{**} of Regions I and II, given, respectively, by [37] and [38], are also plotted along the axial nozzle coordinate in figure 11. The position of the nucleation wave, constructed from states of maximum nucleation, and the flow variables therein seem to be unaltered by transient nucleation effects. This demonstrates the fact that much higher cooling rates than the ones encountered herein (0.3–0.43°C/μs) are needed for an observable change in the position of the nucleation wave and the flow field therein.

5. CONCLUSIONS

In this investigation we have studied transient effects of nucleation on steady-state nucleation rates in both steady and unsteady expansions of a vapor in the metastable state using the relaxation time approximation (RTA). From the general behavior of Gibbs formation energy for the creation of condensation nuclei of critical size along particle paths, we distinguish three regions of nucleation with different characteristic times (or characteristic lengths in steady expansions). In each region the asymptotic expressions for unsteady nucleation rates are given explicitly and the conditions under which transient nucleation effects become unimportant (domain of validity of the steady-state nucleation rates) are displayed. Using the classical steady-state nucleation rate equation together with the asymptotic method for nonequilibrium condensation by Delale *et al.* (1993, 1995), we investigated the influence of transient nucleation effects in shock tube experiments of Barschdorff (1975) and nozzle experiments of Schnerr (1989) for the condensation of water in moist air. For these experiments we find that transient effects on nucleation rates seem to be more

significant as saturation is approached within the validity of RTA. In the expansions along particle paths in the rarefaction wave with initial driver section conditions corresponding to those in the experiments of Barschdorff (1975), we find along particle paths with relatively low cooling rates (0.04–0.28°C/μs) that the position of nucleation wave front (constructed from those states with maximum nucleation rates) and the flow field therein remain essentially unaltered by transient nucleation effects. On the other hand, along particle paths with high cooling rates (e.g. of the order of 3°C/μs or higher) which lie close to the center O where measurements are practically impossible, we theoretically find that transient effects of nucleation begin to influence the position of the nucleation wave front and the flow field therein resulting in a delay for the position of the nucleation wave front and thereby, a decrease in the pressure and temperature therein. For the nozzle experiments of Schnerr (1989) with cooling rates in the range of 0.30–0.43°C/μs under atmospheric supply conditions, we find that the position of the nucleation wave and the flow field therein are essentially unaltered by transient effects of nucleation.

The results presented in this paper show that transient effects of nucleation may influence the macroscopic flow field depending on working fluid and initial conditions, particularly for those expansions with very high cooling rates. Furthermore, when sufficient data for such expansions become available, one can use the asymptotic expressions of the distinct nucleation regions obtained in this article by RTA for the unsteady nucleation rate equation in order to establish a practical criterion as to when transient effects of nucleation are likely to be important. The transient effects of nucleation can also be examined by employing different steady-state nucleation theories. Finally, the asymptotic theory presented herein can be compared with the results of direct molecular simulations (e.g. Monte Carlo methods).

Acknowledgements—This work is supported in part by Deutsche Forschungsgemeinschaft Graduiertenkolleg "Energie- und Umwelttechnik" at the University of Karlsruhe and in part by the Scientific and Technical Research Council of Turkey (TÜBİTAK). The authors would also like to acknowledge fruitful brief discussions with Dr V. A. Shneidman during the Nucleation Symposium (1994) at Stanford.

REFERENCES

Abraham, F. F. 1974 *Nucleation Theory*. Academic, New York.

Andrés, R. P. & Boudart, M. 1965 Time lag in multistate kinetics: nucleation. *J. Chem. Phys.* **42,** 2057–2064.

Barschdorff, D. 1975 Carrier gas effects on homogeneous nucleation of water vapor in a shock tube. *Phys. Fluids* **18,** 529–535.

Becker, R. & Döring, W. 1935 Kinetische behandlung der keimbildung in übersättigten dämpfen. *Ann. Phys.* **24,** 719–752.

Collins, F. C. 1955 Time lag in spontaneous nucleation due to non-steady state effects. *Z. Electrochem.* **59,** 404–407.

Courtney, W. G. 1962 Non-steady state nucleation. *J. Chem. Phys.* **36,** 2009–2017; Kinetics of condensation of water vapor, *ibid* 2018–2025.

Delale, C. F. & Meier, G. E. A. 1993 A semiphenomenological droplet model of homogeneous nucleation from the vapor phase. *J. Chem. Phys.* **98,** 9850–9858.

Delale, C. F., Schnerr, G. H. & Zierep, J. 1993 Asymptotic solution of transonic nozzle flows with homogeneous condensation. I. Subcritical Flows. *Phys. Fluids A* **5,** 2969–2981.

Delale, C. F., Schnerr, G. H. & Zierep, J. 1995 Asymptotic solution of shock tube flows with homogeneous condensation. *J. Fluid Mech.* **287,** 93–118.

Dillmann, A. & Meier, G. E. A. 1991 A refined droplet approach to the problem of homogeneous nucleation from the vapor phase. *J. Chem. Phys.* **94,** 3872–3884.

Erdelyi, A. 1956 *Asymptotic Expansions*. Dover, New York.

Farkas, L. 1927 Keimbildung in übersättigten gebilden. *Z. Phys. Chem.* **125,** 236–242.

Feder, J., Russel, K. C., Lothe, J. & Pound, G. M. 1966 Homogeneous nucleation and growth of droplets in vapours. *Adv. Phys.* **15,** 111–178.

Fisher, M. E. 1967 The theory of condensation and the critical point. *Physics* **3,** 255–283.

Frenkel, J. 1946 *Kinetic Theory of Liquids*. Oxford University Press, Oxford.

Kalikmanov, V. I. & Van Dongen, M. E. H. 1995 Semiphenomenological theory of homogeneous vapor–liquid nucleation. *J. Chem. Phys.* **103,** 4250–4255.

Kantrowitz, A. 1951 Nucleation in very rapid vapor expansions. *J. Chem. Phys.* **19,** 1097–1100.

Kotake, S. & Glass, I. I. 1981 Flows with nucleation and condensation. *Prog. Aerospace Sci.* **19,** 129–196.

Lothe, J. & Pound, G. M. 1962 Reconsideration of nucleation theory. *J. Chem. Phys.* **36,** 2080–2085.

McDonald, J. E. 1963 Homogeneous nucleation in vapor condensation. II. Kinetic aspects. *Am. J. Phys.* **31,** 31–41.

Probstein, R. 1951 Time lag in the self-nucleation of a supersaturated vapor. *J. Chem. Phys.* **19,** 619–626.

Schnerr, G. 1989 2-D transonic flow with energy supply by homogeneous condensation: onset condition and 2-D structure of steady Laval nozzle flow. *Expts Fluids* **7,** 145–156.

Shneidman, V. A. 1987 Size distribution of new-phase particles during transient condensation of a supercooled gas. *Sov. Phys. Tech. Phys.* **32,** 76–81.

Sirovich, L. 1971 *Techniques of Asymptotic Analysis.* Springer, New York.

Volmer, M. 1939 *Kinetik der Phasenbildung.* Steinkopff, Dresden.

Wakeshima, H. 1954 Time lag in the self-nucleation. *J. Chem. Phys.* **22,** 1614–1615.

Zeldovich, Y. B. 1942 Theory of formation of a new phase: cavitation. *J. Exp. Theor. Phys.* **12,** 525.

Zettlemoyer, A. C. 1969 *Nucleation.* Dekker, New York.